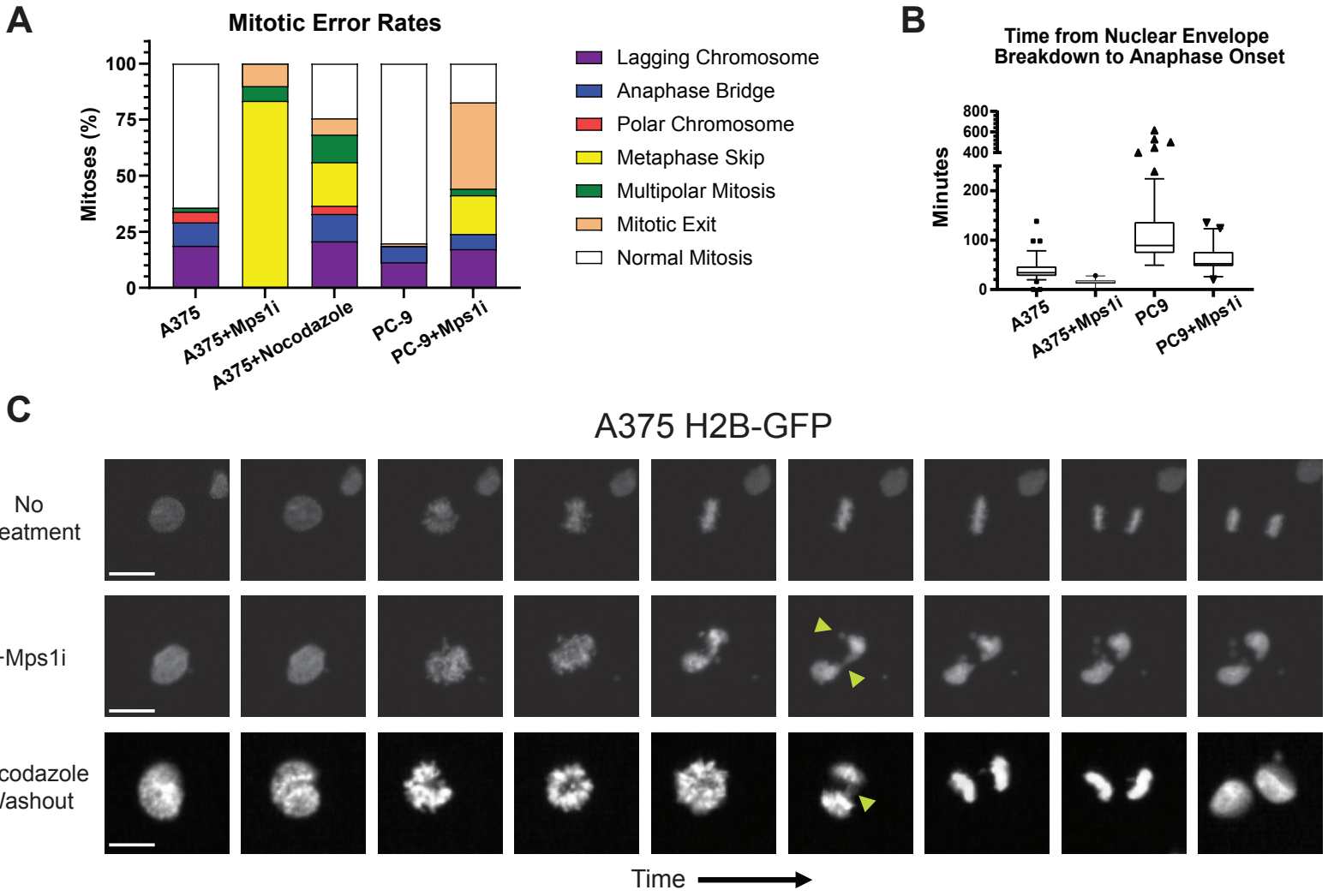

Figure S1. Induction of chromosomal instability by Mps1 inhibitor treatment. Related to Figure 1.

(A) Bar graph of the percent of mitoses in GFP-H2B A375 and PC-9 cells that display various chromosome missegregation events in the presence or absence of the Mps1 inhibitor AZ3146 or after nocodazole washout. Description of mitotic errors listed in Materials and Methods. A375, N = 77; A375 + Mps1i, N = 54; A375 + Nocodazole Washout, N = 82; PC9, N = 45; PC9 + Mps1i, N = 40.

(B) Tukey plot of the duration of time cells spent in mitosis in the presence or absence of AZ3146. Same N as in (A).

(C) Image series of representative mitoses from cells in the presence or absence of AZ3146 or after nocodazole washout. Scale Bar – 10μm.

Figure S2

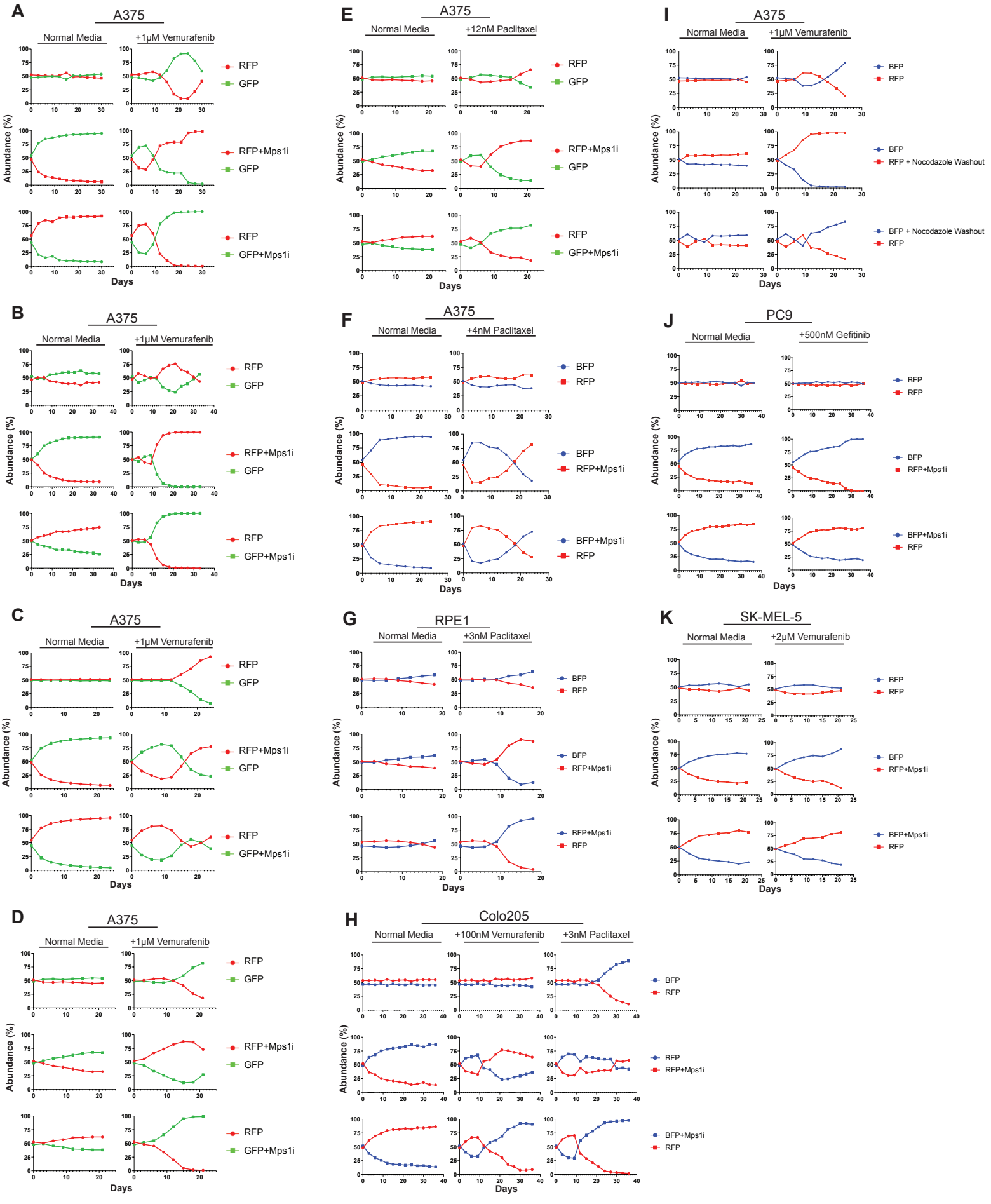
A
A375
Normal Media
+1μM Vemurafenib
RFP
GFP
RFP+Mps1i
GFP
RFP
GFP+Mps1i
Abundance (%)
Days
B
A375
Normal Media
+1μM Vemurafenib
RFP
GFP
RFP+Mps1i
GFP
RFP
GFP+Mps1i
Abundance (%)
Days
C
A375
Normal Media
+1μM Vemurafenib
RFP
GFP
RFP+Mps1i
GFP
RFP
GFP+Mps1i
Abundance (%)
Days
D
A375
Normal Media
+1μM Vemurafenib
RFP
GFP
RFP+Mps1i
GFP
RFP
GFP+Mps1i
Abundance (%)
Days
E
A375
Normal Media
+12nM Paclitaxel
RFP
GFP
RFP+Mps1i
GFP
RFP
GFP+Mps1i
Abundance (%)
Days
F
A375
Normal Media
+4nM Paclitaxel
BFP
RFP
BFP
RFP+Mps1i
BFP+Mps1i
RFP
Abundance (%)
Days
G
RPE1
Normal Media
+3nM Paclitaxel
BFP
RFP
BFP
RFP+Mps1i
BFP+Mps1i
RFP
Abundance (%)
Days
H
Colo205
Normal Media
+100nM Vemurafenib
+3nM Paclitaxel
BFP
RFP
BFP
RFP+Mps1i
BFP+Mps1i
RFP
Abundance (%)
Days
I
A375
Normal Media
+1μM Vemurafenib
BFP
RFP
BFP
RFP + Nocodazole Washout
BFP + Nocodazole Washout
RFP
Abundance (%)
Days
J
PC9
Normal Media
+500nM Gefitinib
BFP
RFP
BFP
RFP+Mps1i
BFP+Mps1i
RFP
Abundance (%)
Days
K
SK-MEL-5
Normal Media
+2μM Vemurafenib
BFP
RFP
BFP
RFP+Mps1i
BFP+Mps1i
RFP
Abundance (%)
Days

Figure S2. Transient CIN can accelerate the acquisition of drug resistance in many but not all contexts. Related to Figures 1 and 2.

(A-D) Relative abundance of competing A375 cell populations +/- vemurafenib.

(E-F) Relative abundance of competing A375 cell populations +/- paclitaxel.

(G) Relative abundance of competing RPE1 cell populations +/- paclitaxel.

(H) Relative abundance of competing Colo205 cell populations +/- vemurafenib, or +/- paclitaxel.

(I) Relative abundance of competing A375 cell populations +/- vemurafenib. Prior to competition, A375 cells were either grown under normal conditions or pretreated with a pulse treatment of nocodazole followed by mitotic shake-off.

(J) Relative abundance of competing PC-9 cell populations +/- gefitinib.

(K) Relative abundance of competing SKMEL-5 cell populations +/- vemurafenib.

Figure S3

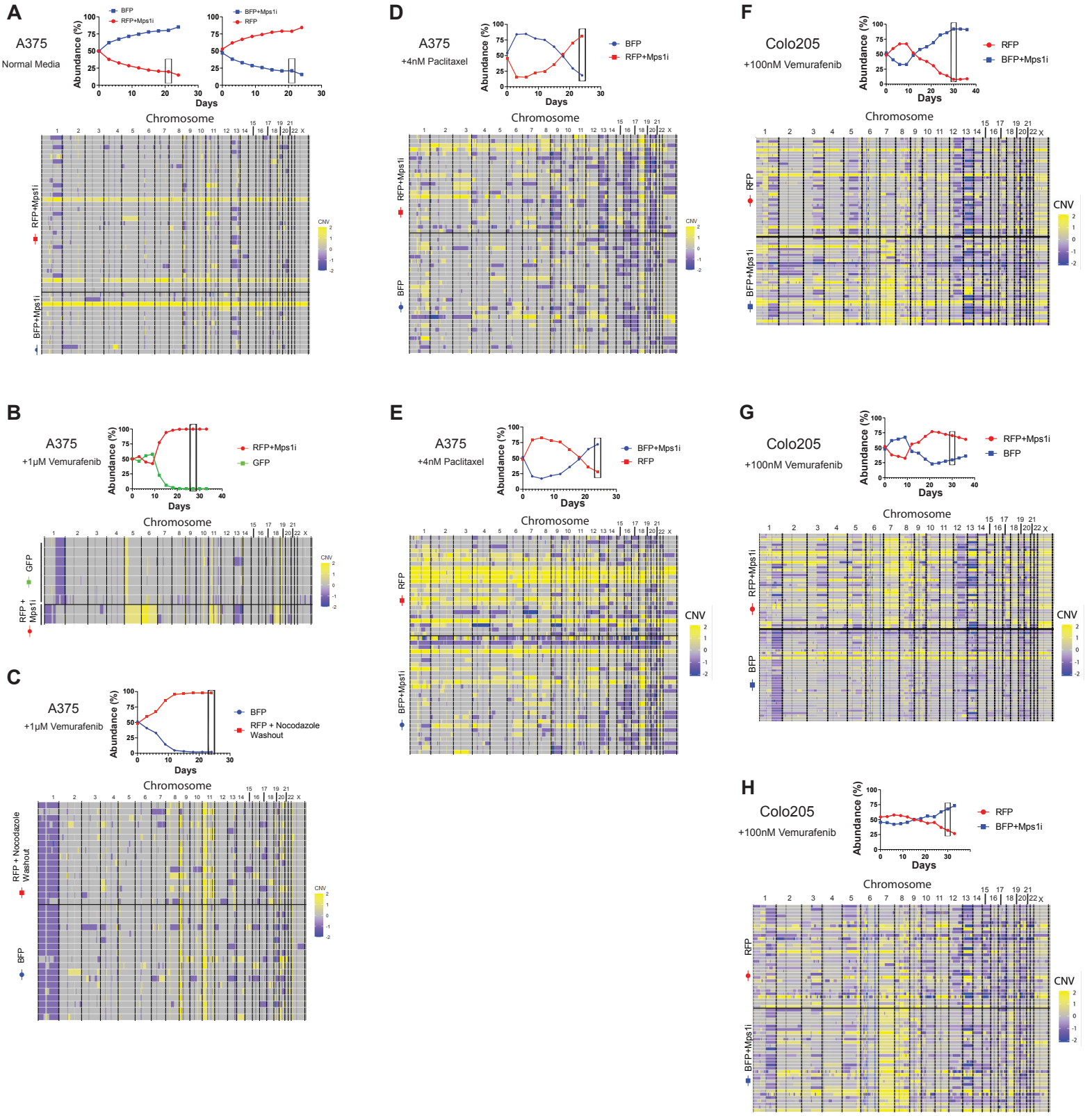
A
A375
Normal Media
BFP
RFP+Mps1i
BFP+Mps1i
RFP
Abundance (%)
Days
Chromosome
RFP+Mps1i
BFP+Mps1i
CNV
B
A375
+1μM Vemurafenib
RFP+Mps1i
GFP
GFP
RFP + Mps1i
C
A375
+1μM Vemurafenib
BFP
RFP + Nocodazole Washout
RFP + Nocodazole Washout
BFP
D
A375
+4nM Paclitaxel
BFP
RFP+Mps1i
RFP+Mps1i
BFP
E
A375
+4nM Paclitaxel
BFP+Mps1i
RFP
RFP
BFP+Mps1i
F
Colo205
+100nM Vemurafenib
RFP
BFP+Mps1i
RFP
BFP+Mps1i
G
Colo205
+100nM Vemurafenib
RFP+Mps1i
BFP
RFP+Mps1i
BFP
H
Colo205
+100nM Vemurafenib
RFP
BFP+Mps1i
RFP
BFP+Mps1i

Figure S3. Additional single-cell sequencing results from competition experiments. Related to Figures 3 and S2.

(A) (Top) Plots displaying the competitions of A375 cells in normal medium from which cells were isolated for single cell sequencing. The boxes indicate the time point when cells were isolated. (Bottom) Heatmap displaying the karyotypic alterations of single cells isolated from the above competition.

(B) (Top) Plot displaying the competition of A375 cells in vemurafenib from which cells were isolated for single cell sequencing. The box indicates the time point when cells were isolated. (Bottom) Heatmap displaying the karyotypic alterations of single cells isolated from the above competition. Note that sequencing for only two Mps1i-treated cells passed our quality control thresholds.

(C) (Top) Plot displaying competition of A375 cells, either untreated or pre-treated with a nocodazole washout, in vemurafenib. Box indicates time point when single cells were isolated for single cell sequencing. (Bottom) Heatmap displaying the karyotypic alterations of single cells isolated from the above competition.

(D-E) (Top) Plot displaying the competition of A375 cells in paclitaxel from which cells were isolated for single cell sequencing. The box indicates the time point when cells were isolated. (Bottom) Heatmap displaying the karyotypic alterations of single cells isolated from the above competition.

(F-H) (Top) Plot displaying the competition of Colo205 cells in vemurafenib from which cells were isolated for single cell sequencing. Box indicates time point when cells were isolated. (Bottom) Heatmap displaying the karyotypic alterations of single cells isolated from the above competition.

N.B. – Competition plots shown in (A) were previously shown in Figure 1B, and were a part of the same set of competition experiments shown in Figure 3B. The competition plots shown in (B), (C), (D-E), (F-G), and (H) were previously shown in Figures S2B, S2I, S2F, S2H, and 2B, respectively.

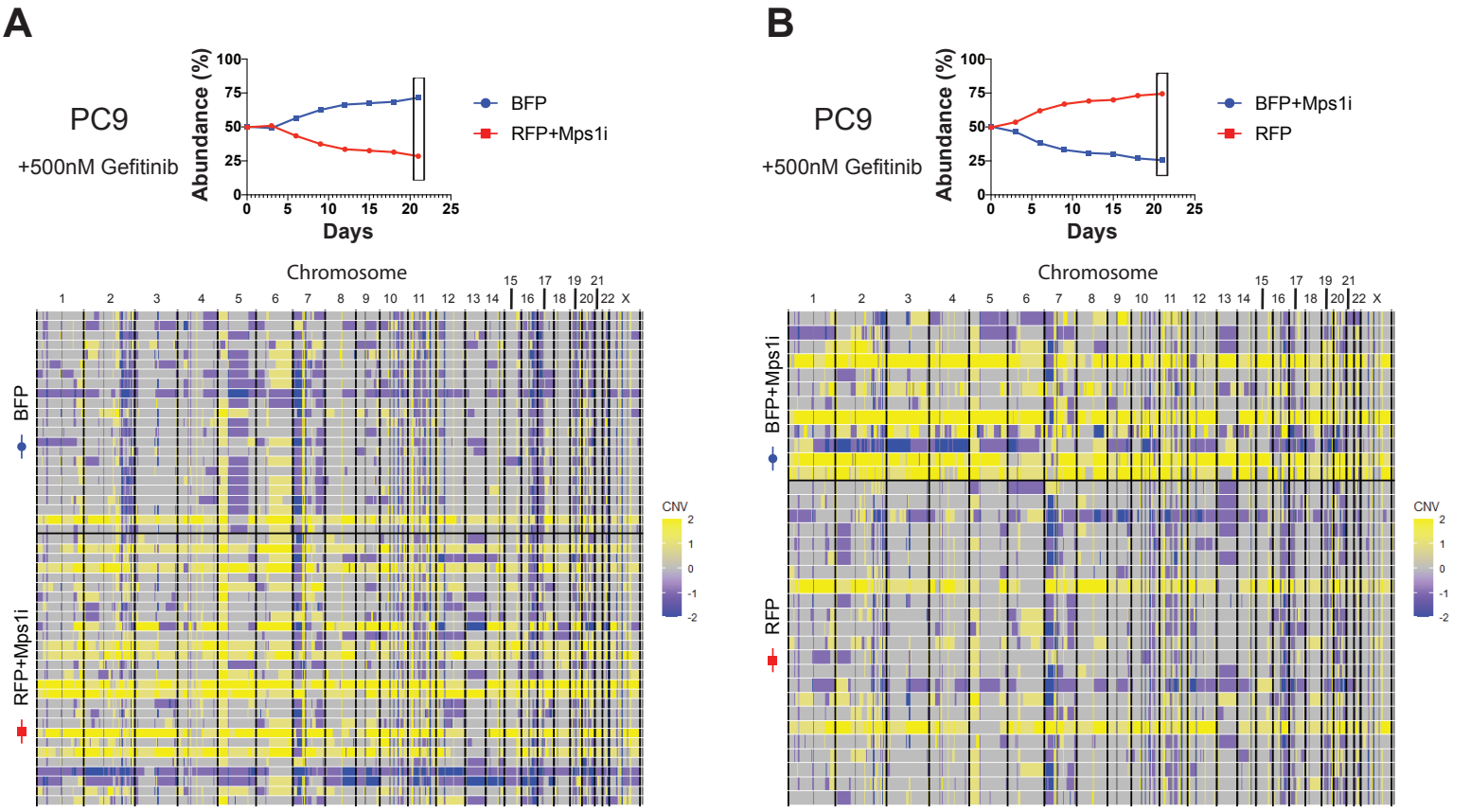

Figure S4. Single-cell sequencing identifies recurrent whole-genome duplications in Mps1i-treated PC9 cells. Related to Figure 3.

(A-B) (Top) Plot displaying the competition of PC9 cells in gefitinib from which cells were isolated for single cell sequencing. Box indicates time point when cells were isolated. (Bottom) Heatmap displaying the karyotypic alterations of single cells isolated from the above competition.

A

Cell Population	BRAFi Resistance Mutation Detected?							
	NRAS	BRAF	MEK1/2	RAC1	NF1	PTEN	RB1	STAG2/3
Parental 2	X	$BRAF^{V600E}$ Only	X	X	X	X	X	X
Pulse-Mps1i	X	$BRAF^{V600E}$ Only	X	X	X	X	X	X
BFP Competition 1	X	$BRAF^{V600E}$ Only	X	X	X	X	X	X
BFP Competition 2	X	$BRAF^{V600E}$ Only	X	X	X	X	X	X
RFP Competition 1	X	$BRAF^{V600E}$ Only	X	X	X	X	X	X
RFP Competition 2	X	$BRAF^{V600E}$ Only	X	X	X	X	X	X
BFP+Mps1i Competition 1	X	$BRAF^{V600E}$ Only	X	X	X	X	X	X
BFP+Mps1i Competition 2	X	$BRAF^{V600E}$ Only	X	X	X	X	X	X
RFP+Mps1i Competition 1	X	$BRAF^{V600E}$ Only	X	X	X	X	X	X
RFP+Mps1i Competition 2	X	$BRAF^{V600E}$ Only	X	X	X	X	X	X

B

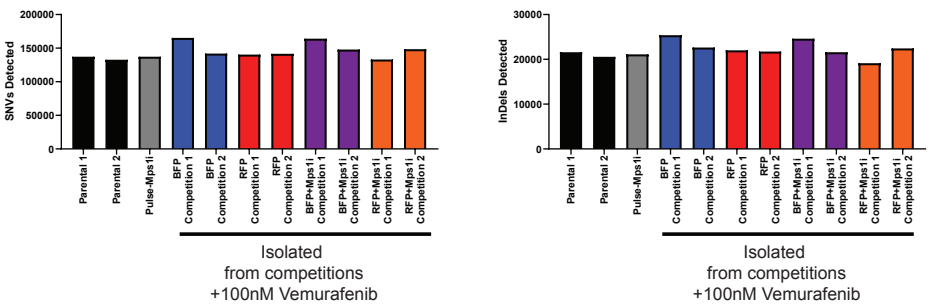

C

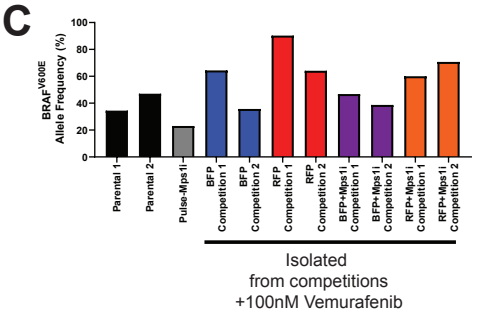

D

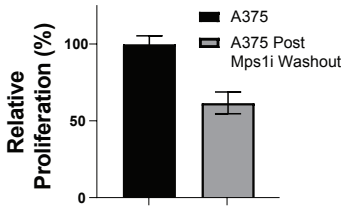

E

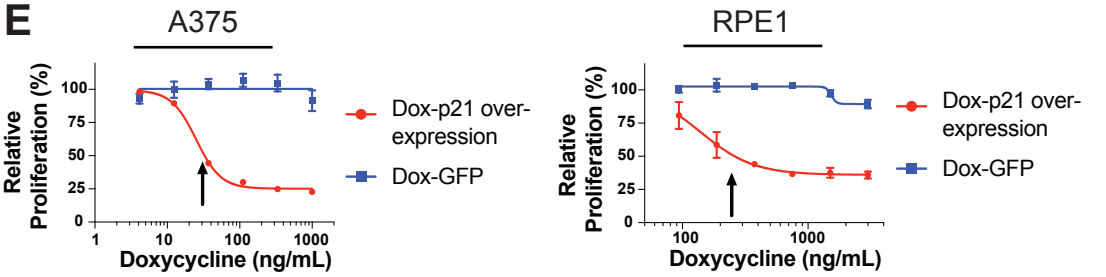

F

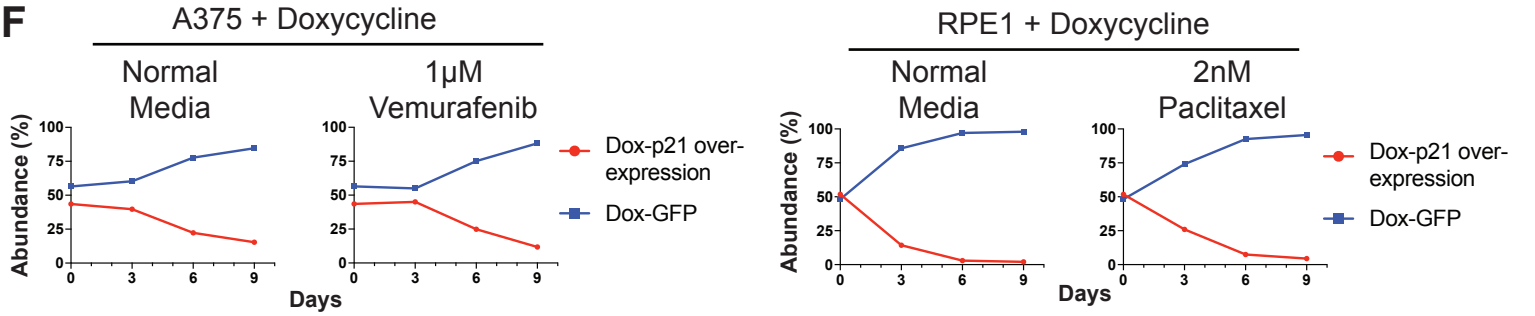

Figure S5. Assessment of alternative causes of resistance. Related to Figures 3 and S2.

(A) Table summarizing whole-exome sequencing data of Colo205 cells collected from competitions in vemurafenib. Genes that have previously been associated with BRAFi resistance are displayed. An "X" indicates that no mutations were found in this gene that are absent from the non-BRAFi-treated parental cell populations. Note that, as expected, $BRAF^{V600E}$ was detected in all samples.

(B) Bar graphs displaying number of InDels and SNVs detected in Colo205 cells collected from competitions in vemurafenib.

(C) Bar graph of $BRAF^{V600E}$ allele frequency in Colo205 cells collected from competitions in vemurafenib.

(D) Bar graph showing decreased proliferation in A375 cells post Mps1i washout. N = 3.

(E) Doxycycline dose-response curves of A375 and RPE1 cells transduced with vectors for the inducible expression of a fluorophore (Dox-GFP) or p21 (Dox-p21 overexpression). Arrows indicate doxycycline doses selected to recapitulate the cell cycle delay induced by Mps1i treatment. N = 3.

(F) Relative abundance of A375 and RPE1 cells competed in the indicated conditions. Cells harbor vectors for the doxycycline inducible expression of a fluorophore (Dox-GFP) or p21 (Dox-p21 overexpression). Plots shown are representative of 3 replicate competitions.

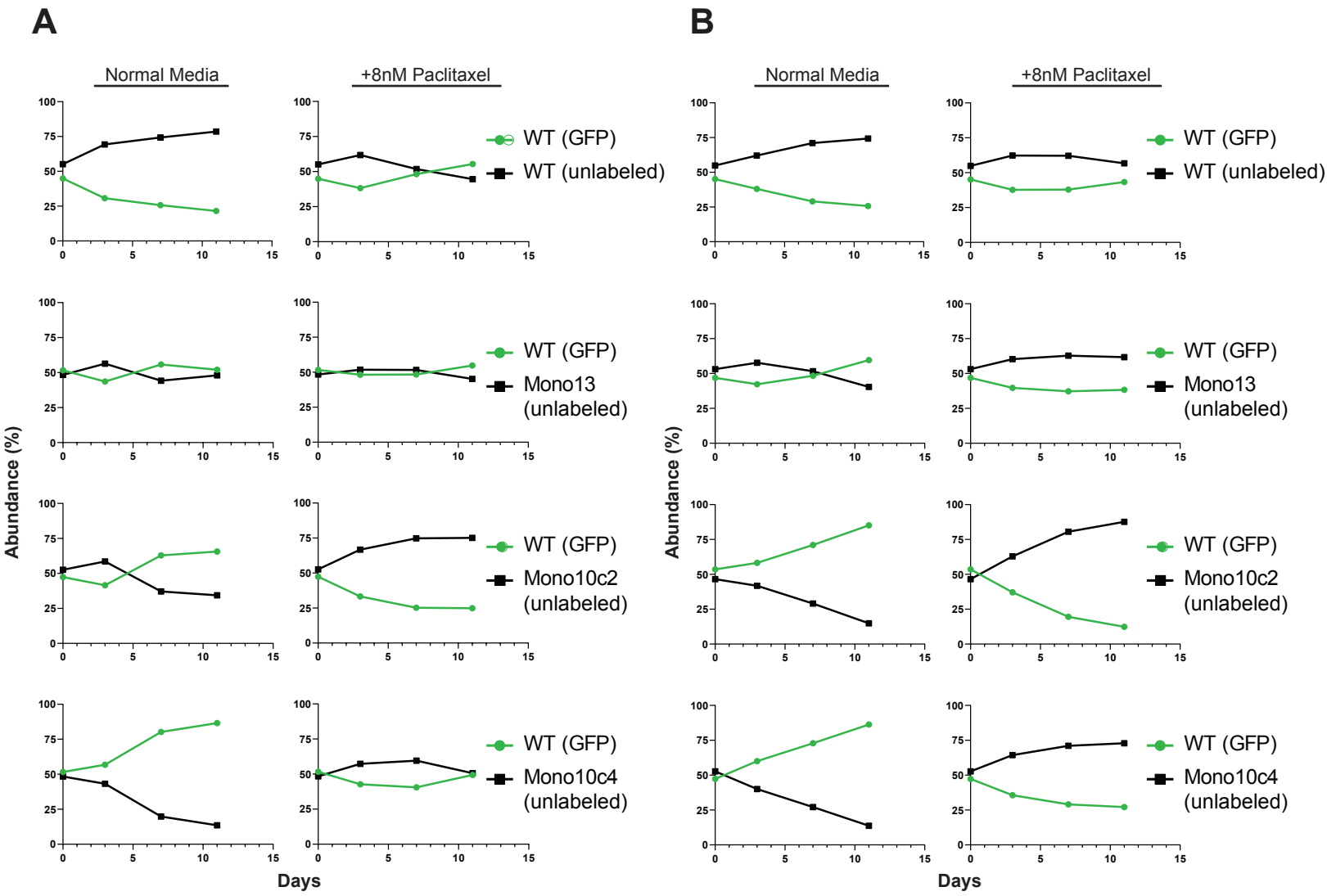

Figure S6. A recurrent aneuploidy recovered in cellular competition experiments is sufficient to confer resistance to paclitaxel in multiple replicates. Related to Figure 4.

(A-B) Replicates of the experiment presented in Figure 4: relative abundance of GFP-expressing RPE1 cells competed against unlabeled monosomies under normal growth conditions or in the presence of paclitaxel.